Sustainable Cities and Society 32 (2017) 547–556

Contents lists available at ScienceDirect

Sustainable Cities and Society

journal homepage: www.elsevier.com/locate/scs

Urban grid forms as a strategy for reducing heat island effects in arid cities

María Belén Sosa*, Erica Norma Correa, María Alicia Cantón

Instituto de Ambiente, Hábitat y Energía (INAHE) – Consejo Nacional de Investigaciones Científicas y Técnicas (CONICET) – CCT Mendoza, Argentina

ARTICLE INFO

Keywords:
Urban grids
Urban heat island
Thermal behavior
Arid cities
Planning
Energy consumption

ABSTRACT

The urban heat island (UHI) modifies the thermal behavior of cities. UHI effects increase the demand for electricity and decreases the livability of outdoor and indoor spaces. This paper seeks to identify forms of urban grids (UGs) that contribute to the reduction of the UHI in Mendoza-Argentina. The microclimates of 10 urban canyons (UCs) were monitored, analyzed and compared during the summertime. This investigation considers the thermal behaviors of open-forested and compact-non forested streetscapes using 4 UG forms. The data were statistically analyzed. The results suggest that the minimum air temperature is related to the combined effects of the neighborhood grid and the UC configuration. However, the maximum and average air temperatures are related to the UC configuration. The multi-azimuthal UG remains cooler. Additionally, the compact-non forested UC was found to be the hottest, which differs from what is known concerning the thermal behavior of UC configurations in the arid zone. When this streetscape is compared to the open-forested UCs, air temperatures differ up to 10.2 °C during the afternoon, 1.7 °C at night, and buildings consume up to 65% more electricity. In summary, creating thermally efficient cities in arid zones requires using the best combination of UG forms and UC design.

1. Introduction

Urban populations have been growing worldwide; presently, half of the world's population resides in urban areas (UN-Habitat, 2016). Consequently, the land area occupied by cities has increased, as has energy consumption. By 2030, global demand for energy is expected to grow by 40–50% (UN-Habitat, 2016).

The process of urban planning is closely related to climate, given that the central purpose of planning is to create an environment suited for humans (Zhao, Fu, Liu, & Fu, 2011). The design and use of the built environment impacts humans at different scales: macro-scale (global warming) and micro-scale (alteration of the urban climate). One of the main alterations of the urban climate is the increase of air temperature, which creates the urban heat island (UHI) phenomenon (Oke, 1982). Research has shown that UHI is primarily caused by the built environment in urban areas in which natural areas are replaced with a high concentration of impervious surfaces that have triggered many environmental issues (Ahmed, Kamruzzaman, Zhu, Shahinoor Rahman, & Keechoo, 2013).

This work focuses on the Mendoza metropolitan area (MMA), which is located in central western Argentina (32°53°S, 68°51°W, 750 m. a. s. l.) in an arid continental climate with low percentages of relative atmospheric humidity and high heliophany. Cities at a global scale usually present one of the two types of streetscapes: compact or open. The compact model has continuous urban development, consisting of tall buildings and narrow streets where the use of urban forestation is absent or scarce. In contrast, the open model—the area studied—has lower buildings with wide and forested streets (Correa, Ruiz, & Cantón, 2010).

Since 2003, the INAHE-CONICET has been studying the urban climate of the MMA with a focus on the magnitude, causes and consequences of the UHI. In arid cities, the UHI is perceived with greater intensity during summertime nights. Previous studies have established some of the impacts caused by this phenomenon: an increase of up to 20% in energy consumption for air conditioning, as well as worsened outdoor thermal comfort conditions (Correa, de Rosa, & Lesino, 2008; Ruiz & Correa, 2014). For example, in the summer of 2014, an intense heat wave caused an increase of air temperature to over 40 °C in the MMA. In response to the heat, air conditioning equipment was used intensively to create indoor thermal comfort. This demand reached record levels of electric energy consumption, with an increase approximately 11.5% between January 2014 and January 2013 (EPRE, 2014).

Many studies suggest that urban planning can influence urban temperature. Jusuf, Wong and Hagen (2007) demonstrate that appropriate planning of land use can mitigate the effects of UHI and improve comfort levels. These points are of interest for developing countries that are undergoing rapid urbanization (Wu, 2014). Shahraki et al. (2011)

* Corresponding author.
E-mail address: msosa@mendoza-conicet.gob.ar (M.B. Sosa).

http://dx.doi.org/10.1016/j.scs.2017.05.003
Received 23 September 2016; Received in revised form 2 May 2017; Accepted 3 May 2017
Available online 10 May 2017

estimate that the urban sprawl rate is close to three times the population growth observed for the same period. The results from Minghong and Xiubin (2015) showed that UHI increases with the city growth (i.e., for a city size > 2 km^2, 60% of the UHI variance occurs during the night). Additionally, Stone, Hess and Frumkin (2010) found that the rate of increase in the number of extreme heat events in the most sprawling metropolitan regions was more than double the rate of the observed increase in the most compact metropolitan regions. Finally, Jo, Goleen and Shin (2009) showed higher surface temperatures are linked with a decreased level of vegetation, illustrating the impact of the built environment on urban climate change.

Regarding urban morphology, researchers often focus on urban canyons (UCs). In built environments, UCs usually compose more than a quarter of urbanized areas (Shashua-Bar and Hoffman, 2003); or in some historically planned cities, such as Manhattan or Barcelona, this area is up to 30% of their built surface (UN-Habitat, 2013). Worldwide, there are many studies that discuss strategies of how geometry, materiality and the forestation of UCs can mitigate UHI (Alchapar and Correa, 2015; Lin, Matzarakis, & Hwand, 2011; Ruiz, Sosa, & Cantón, 2015; Sanusi, Johnstone, May, & Livesley, 2016; Shashua-Bar & Hoffman, 2003). However, there is not enough research that considers how planning strategies related to the morphologies of low-density residential neighborhoods can contribute to cooling urban air temperatures. In this sense, Middel, Häb, Brazel, Martin and Guhathakurta (2014) have demonstrated, at the neighborhood scale, that the urban form has a larger impact on daytime temperatures than urban greening. Additionally, Middel, Chhetri and Quay (2015), assessed the combined cooling benefits of trees and cool roofs at this scale. They have demonstrated that a 25% increase of tree canopy in residential neighborhoods resulted in an average decrease of 2.0 °C during the day, whereas cool roofs showed a reduction of only 0.3 °C of air temperature.

Finally, the increase of extreme heat events and their consequences of overheating outdoor and indoor air temperatures have significant implications for energy consumption, thermal comfort and the health of city dwellers. Lin et al. (2011) determined that a 1 °C increase in temperature increases peak electricity demands by 2–4% when temperatures exceed 15–20 °C. Further, it was demonstrated that the extended use of air conditioning increases air temperature by 1 °C in hot-dry cities at night (Salamanca, Georgescu, Mahalov, Moustaoui, & Wang, 2014). This temperature increase generates an additional electricity demand for air conditioning causing a vicious cycle that impacts urban sustainability in a negative way (Wong & Siu-Kit, 2013).

2. Objectives

Within this context, the study has the following objectives:

- To analyze and compare the thermal behaviors of urban canyons located in different urban neighborhood grids;
- To evaluate the impact of different forms of urban neighborhood grids on outdoor temperatures to reduce the UHI effect in the MMA;
- To quantify the impact of urban design decisions on energy consumption for cooling the interior of houses within the assessed urban neighborhoods.

3. Methodology

3.1. Study sites: selection criteria and characterization

The MMA comprises 6 districts: Mendoza Capital, Guaymallén, Las Heras, Godoy Cruz, Maipú and Luján, see Fig. 1. In the MMA, 62.8% of the population lives within these districts, and in the past decade, this percentage has increased by 9.4% (INDEC, 2010). The building density of these districts is considered low because it is constituted mostly of single-family detached houses (IPV, 2010). The selection process of the case studies was categorized into three urban levels: urban districts, urban neighborhood grids and urban canyons.

3.1.1. Urban districts

According to the most recent demographic census, the majority of inhabitants live among the three districts that border the Capital: Guaymallén (16%), Las Heras (12%), and Godoy Cruz (11%). However, in the past decade, the population in the Capital (6%) has declined by 1%. This is an indicator of how the city has been expanding its built boundaries.

Defining and measuring urban forms is not a simple task. In this study, we made a graphic survey to characterize the MMA block geometries of the most populated districts. These urban blocks were classified and quantified using AutoCAD software and separated into four types: (i) square, (ii) rectangular oriented North-South, (iii) rectangular oriented East-West and (iv) irregular. The selection of these geometrical classifiers derives from the MMA urban regulation policies (Regulatory law n°4341/1978). Graphic survey results are detailed in Fig. 1, where the blocks are color coded and the percentages of the four types are presented. It should be noted that the blocks in the Capital are not quantified because the most representative form is the square (Stocco, Cantón, & Correa, 2013).

By analyzing the data of Fig. 1, it can be concluded that the most representative block form of Godoy Cruz is the rectangular type in both orientations (31%). Otherwise, in Guaymallén, the most representative block is irregular (48%); and, finally, in Las Heras, irregular blocks are the most representative (33%) followed by the rectangular ones with a North-South orientation (30%).

3.1.2. Urban neighborhood grids

According to Marshall (2005), an urban grid is a set of streets and blocks that constitute an urban area. Particularly for this study, we highlight 4 types of urban grids at the neighborhood level. Based on the most representative block forms from the graphic survey, four neighborhoods were selected:

- For Godoy Cruz, a neighborhood with rectangular blocks is selected. The key characteristic of this case is to have streets with slight orientation changes (Multi-azimuthal grid − Case 1)
- For Guaymallén, a neighborhood with irregular blocks oriented East-West is selected. The defining characteristic of this case are streets with one inlet/outlet (Cul-de-Sac grid − Case 2)
- For Las Heras, a neighborhood with rectangular blocks oriented North-South and East-West is selected (Rectangular grid − Case 3)
- For Capital, a neighborhood with compact-non forested and open-forested urban canyons is selected. The atypical compacted UC has a narrow street (5.5 m) and no trees, while the two adjoining streets are considered as having a typical open-forested configuration (Reticular grid − Case 4)

The selected grids differ in shape and orientation but maintain certain concrete features that can be compared to identify which forms have better thermal behavior. These reliable urban characteristics can be grouped into two categories: (i) environmental (low-density residential areas) and (ii) the characteristics of neighborhood (i.e., percentages of blocks, streets, built-up areas, compactness ratio and average albedos of streets, sidewalks and façades). Fig. 2 shows the values of the indicators used for the characterization of each selected neighborhood.

Additionally, each neighborhood is classified and characterized according to the study of Stewart & Oke (2012), Local Climate Temperature Zones for Urban Studies (LCZ). According to the LCZ classification, three cases (neighborhoods 1, 2 and 3) correspond to the open-low rise class with scattered trees subclass (LCZ 6b). The neighborhood selected in the Capital district has a mixed class because one of the

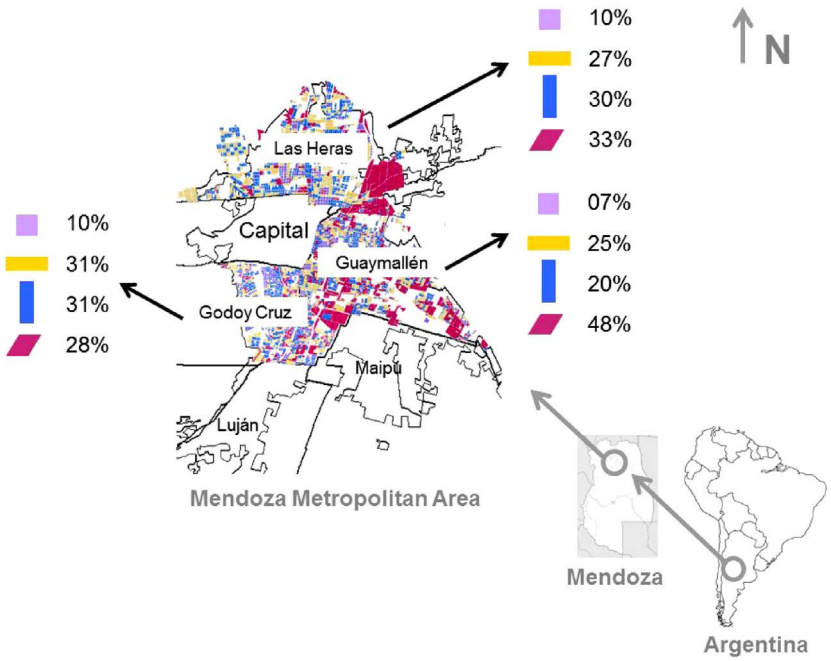

Fig. 1. Types and quantity of urban blocks in each analyzed district of the MMA.

urban canyons (4.c) corresponds to the compact-low rise class (LCZ 3).

3.1.3. Urban canyons

Within each urban neighborhood, the most representative urban canyons (UC) were selected. In these UC, microclimates were monitored. For the multi-azimuthal grid, case 1, two blocks were selected. In the Cul-de-Sac grid, case 2, one block with an East-West orientation was selected. In the rectangular grid, case 3, four blocks were selected with different orientations and lengths (3 blocks with a North-South orientation and 1 with an East-West orientation). Finally, in the

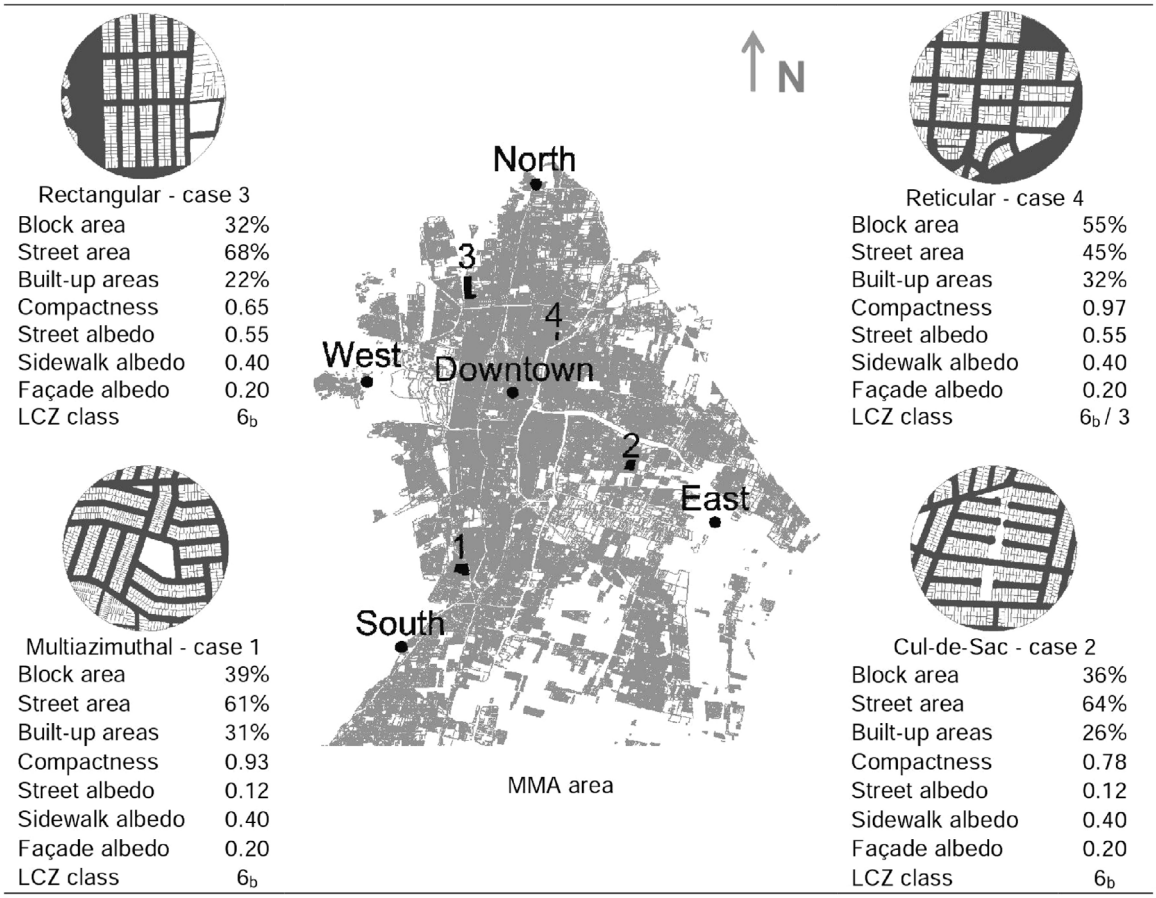

Fig. 2. Indicator values of the urban grids and their location within the MMA.

	Multi-azimuth		Cul-de-Sac	Rectangular				Reticular		
Neighborhood grid and urban canyon designation				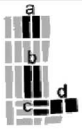						
	1.a	1.b	2	3.a	3.b	3.c	3.d	4.a	4.b	4.c
Length (m)	255	226	145	128	192	83	81	116	110	112
Height (m)	3	3	3	3	3	3	3	3	3	3
Width (m)	20	20	20	16	16	20	20	20	20	5.5
H/W	0.15		0.15	0.19		0.15		0.15		0.55
	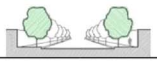		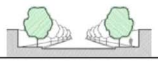	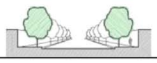				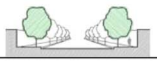		
Street surface (Length x Width) (m^2)	5100	4520	2900	2048	3072	1660	1620	2320	2200	616
Azimuth (°)	146	193	81	181	181	92	184	89	89	85
Orientation axis (°)	E-W	E-W	E-W	N-S	N-S	E-W	N-S	E-W	E-W	E-W
Built-up volume (m^3)	11280	10320	6720	4800	7680	3840	3840	5040	4560	5280
Sky view factor	0.69	0.60	0.57	0.27	0.35	0.61	0.46	0.16	0.50	0.74
										
Quantity of trees (u)	53	52	36	44	53	21	23	31	24	0
Tree specie	*Morus alba*		*Ulmus umbraculifera*	*Morus alba*				*Tipuana tipu*		-

Fig. 3. Descriptor and indicator values of the urban canyons.

reticular grid, case 4, three blocks were selected. In this case, compact and open urban canyon configurations were contrasted (1 block is a compact non-forested and the other 2 are open-forested). Fig. 3 shows the values of the twelve indicators and descriptors that were used to characterize the ten UCs.

The sky view factor (SVF) was calculated from hemispherical images captured with a Nikon® CoolPix digital camera equipped with a fisheye lens and then processed with Pixel de Cielo 1.0 software (Córica & Pattini, 2009). Fig. 4 illustrates the criteria and stages of the selection of study cases.

3.2. Microclimate monitoring

The microclimatic data were obtained from a 34-day measuring campaign from January 8, to February 10, 2014. A fixed sensor-type logger (H08-003-02; HOBO®; Cape Cod, MA) was installed in each urban canyon, at 2 m height above ground, in a solar radiation shield to prevent irradiation and ensure adequate air circulation (Oke, 2004). The sensors recorded data every 15 min. Data were averaged hourly using Excel® software. By analyzing the data, January 15 is selected because the meteorological conditions are replicated for 74% of the total measured period. It is a typical summer day for an arid region (high temperatures, no clouds, moderate wind, low relative humidity, no precipitation) (Weather Underground, 2014). Additionally, a silicon pyrometer (S-LIB-M003; HOBO®; Cape Cod, MA) mounted on a bracket in each canyon at 2 m height above ground was installed. Both sensors were positioned at the center of each urban canyon cross-section. They were mounted to a wood mast on the sidewalks (for the East-West-oriented canyons, the mast was on the North side, and for the case of the North-South-oriented canyons, the sensors were on the West side). Specifically, the silicon pyranometer was mounted level on the top of a bracket positioned in an exposed spot to avoid shadow. Table 1 shows the specification of the measurement devices, and Fig. 5 shows the sensor positions in the urban canyons.

In addition, and following the same methodology, four peripheral or boundary points (North, West, South and East) and a point in the downtown area of the city were monitored during the same period to have a better understanding of how the built environment impacts air temperature (UHI effect). The location of each point is illustrated in Fig. 2.

3.3. Correlation analysis

To define the key variables (urban indicators) that influence the thermal behavior of urban neighborhoods and urban canyon forms (both study scales), a Pearson's correlation coefficient was employed.

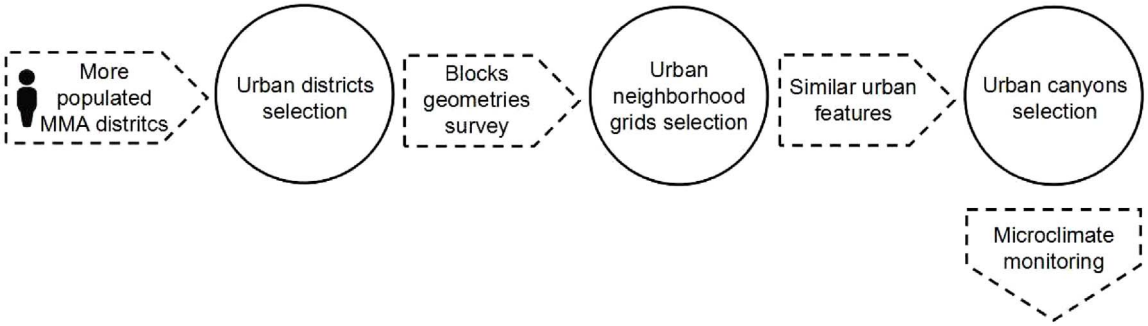

Fig. 4. Criteria and stages of the selection of study cases.

Table 1
Specifications of the measurement devices.

Device	Variable	Measure range	Accuracy	Resolution
H08-003-02	Air temperature	−20 °C to +70 °C	± 0.7 °C at +21 °C	0.4 °C at +21 °C
S-LIB-M003	Solar radiation	0 to 1280 W/m^2	± 10 W/m^2 or ± 5%	1.25 W/m^2

We found that this coefficient is suitable for the analysis because it refers to the extent to which the variables have a linear relationship with each other. The coefficient values were calculated using InfoStat software (Di Rienzo et al., 2011) by using the same correlation matrix for all the urban indicators. Correlation values are presented below in the results section (Table 3).

3.4. Estimation of energy consumption

According to the study aims, we estimated the demand of auxiliary energy (Qaux) for cooling the houses in the monitored UCs. Dynamic simulation tools (DOE-2, Energy Plus) can predict the Qaux consumption for thermal conditioning. However, the use of these tools requires a building reconstruction to compare different design alternatives (morphological and material characteristics) (Maile, Fischer, & Bazjanac, 2007; Rodrigues et al., 2015). In this study, the Qaux assessment seeks to quantify the impact that the neighborhood grids and urban canyon forms have over the energy consumption for cooling the interior of the houses in the study sites under consideration.

Therefore, for the purposes of this investigation, a simplified tool was chosen. PREDISE freeware is used for the pre-design stage (diagnosis phase). This freeware calculates the average indoor temperature and the energy fluxes that the total volume of a building exchanges with the environment through all its exposed surfaces in a steady state in a short period of time (immediate). The energy balance equations used give a first approximation of the impact that the outdoor conditions have on the indoor thermal behavior. Additionally, PREDISE freeware serves as support to be used by other detailed programs through its independence from commercial applications (Hernández, 2002). It was developed by the INENCO research group, the Science department at the National University of Salta, Argentina (download link: http://www.unsa.edu.ar/alejo/predise/).

3.4.1. PREDISE database

PREDISE requires a geographical, meteorological, building and internal heat gains database to function. Geographical data identifies the study site. Meteorological data include air temperature and horizontal solar radiation, which were obtained from the microclimate monitoring campaign following the earlier described methodology. Building data include the material characteristics of all the exposed surfaces (roof, walls, windows and doors). For this study, urban neighborhoods with similar house types were chosen to prevent the incidence of the built-up characteristics (Fig. 6). Finally, the data of internal heat gains reflects the average consumption of a four-person family household (1 man, 1 woman, 2 children) with their electrical and natural gas appliances. The input parameters and values of the PREDISE database are presented in Table 2. The meteorological parameters used are from the coolest (open-forested, case 1.b) to the warmest (compact-non forested, case 4.c) urban canyons.

3.4.2. PREDISE calculation equations

First, PREDISE calculates the heat load unit (CTU) using the following expression:

$$CTU = Qp + Qt + Qv + Qpt + Qi \quad (1)$$

where Qp are the wall energy exchanges, Qt are exchanges through the roof, Qv are the window exchanges, Qpt are the foundation exchanges and Qi are the infiltrations.

Then, the amount of direct solar gains throughout the windows is estimated using the following equation:

$$Qsolar = Ctv \times CTm \times H \times Sv \quad (2)$$

where CTv is the coefficient of the glass transmittance (0.85), CTm is a correction factor that considers the influence of the window frames on the effective area of radiation (0.80), H is the sum of daily solar radiation on the vertical plane in each window (values differ according to the existing solar obstructions on every urban canyon, and they were calculated using Geosol, v2.0), and Sv is the total area of windows.

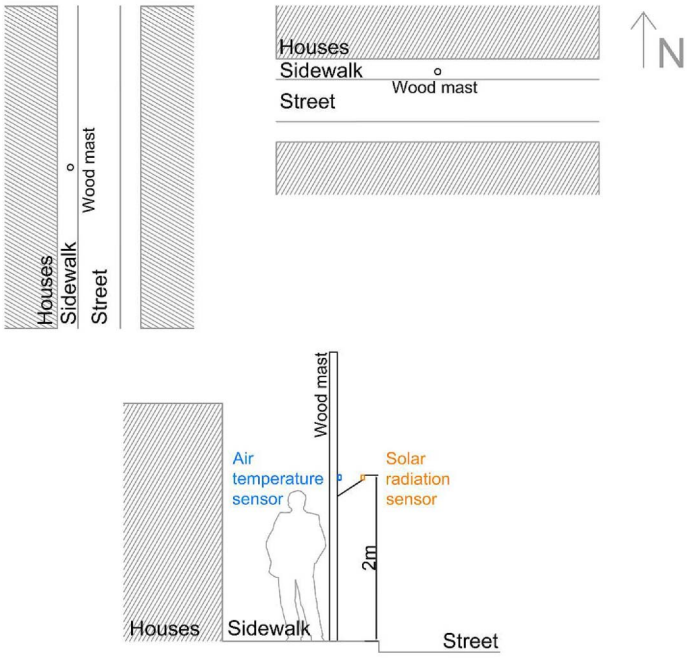

Fig. 5. Sensor positions in the monitored urban canyons.

Fig. 6. Types of houses in each urban neighborhood.

Table 2
PREDISE database parameters and values.

Geographical data	Latitude	−32.5	
	Altitude (m.a.s.l)	746	
	Albedo	0.2	
Meteorological data	Case	Open-forested (1.b)	Compact-non forested (4.c)
	Maximum temperature (°C)	37,5	47,7
	Average temperature (°C)	31,6	34,1
	Horizontal solar radiation (MJ/m^2)	28	30
Building data	Building volume (m^3)	240	
	Building area (m^2)	80	
	Roof material	concrete slab	
	Roof area (m^2)	80	
	Insulation	expanded polystyrene (λ= 0.03 W/m°C of 0.10 m thick)	
	Wall material	solid brick (0.20 m thick)	
	Wall area (m^2)	180	
	Foundation perimeter (m)	80	
	Door material	wood	
	Door area (m^2)	2.2	
	Total window area (m^2)	6	
	Window azimuth	0/180/270	
	Air infiltration (renovations per hour)	2	
	Interior average temperature (°C)	25	
Internal heat gains	People (MJ/day)	29	
	Electrical appliances (MJ/day)	8	
	Natural gas appliances (MJ/day)	25	

Finally, the Qaux is deduced from the following energy balance equation:

$$CTU = (T°int - T°ext) - Qsolar - Qgen = Qaux \quad (3)$$

where T°ext is the exterior average temperature, T°int is the interior average temperature, and Qgen is the internal heat gains.

Table 3
Pearson correlation values.

Variables		Maximum (r)	Minimum (r)	Average (r)
Neighborhood	Block area	0.06	−0.65*	−0.17
	Street area	−0.06	0.65*	0.17
	Built-up area	0.12	−0.46	−0.14
	Compactness ratio	0.12	−0.46	−0.14
Urban canyon	Length	−0.34	−0.54*	−0.31
	Width	−0.81*	−0.50*	−0.82*
	H/W	0.86*	0.37	0.76*
	Street surface	−0.59*	−0.70*	-0.60*
	Azimuth	−0.45	0.02	−0.33
	Built-up volume	−0.28	−0.61*	−0.33
	SVF	0.51*	−0.53*	0.24
	Quantity of trees	−0.70*	−0.33	−0.49

* Significant values (a = 0.05).

4. Results

The data of the microclimate monitoring were analyzed in 3 stages: (i) thermal behavior of urban canyons located in different urban neighborhood grids; (ii) thermal behavior relationships between urban neighborhood grids, downtown and peripheral points; and (iii) influence of the urban form on the energy consumption for cooling within the assessed urban neighborhoods.

4.1. Thermal behavior of urban canyons located in different urban neighborhood grids

Fig. 7 shows the thermal behaviors (maximum, minimum and average temperature) of each UC for the day studied (January 15, 2014). In this study, we focus on three attributes. Maximum air temperatures were analyzed because they are one of the factors that determine the outdoor habitability, minimum air temperatures were chosen since they give insight into UHI intensities, and average air temperatures were considered since they are related to the energy consumption needed for cooling.

The results summarized in Fig. 7 show that:

- In the multi-azimuthal grid: (i) during the heating period (8am − 8pm), UC 1.a is 2 °C warmer than 1.b, and (ii) during the cooling period (8pm − 8am), the minimum air temperature is similar in

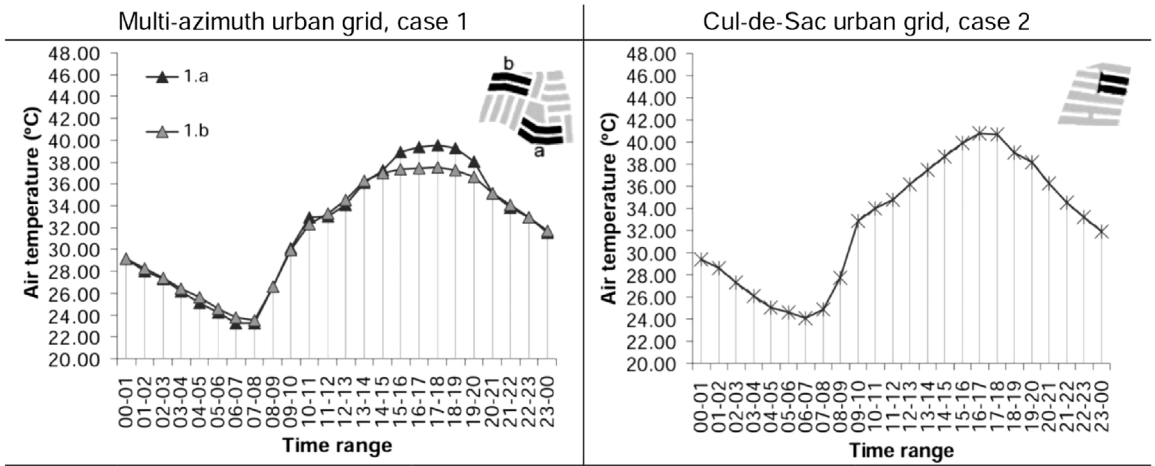

Case	Maximum	Minimum	Average
1.b	37.5°C	23.5°C	31.6°C
1.a	39.5°C	23.2°C	31.9°C

Case	Maximum	Minimum	Average
2	40.8°C	24.1°C	32.8°C

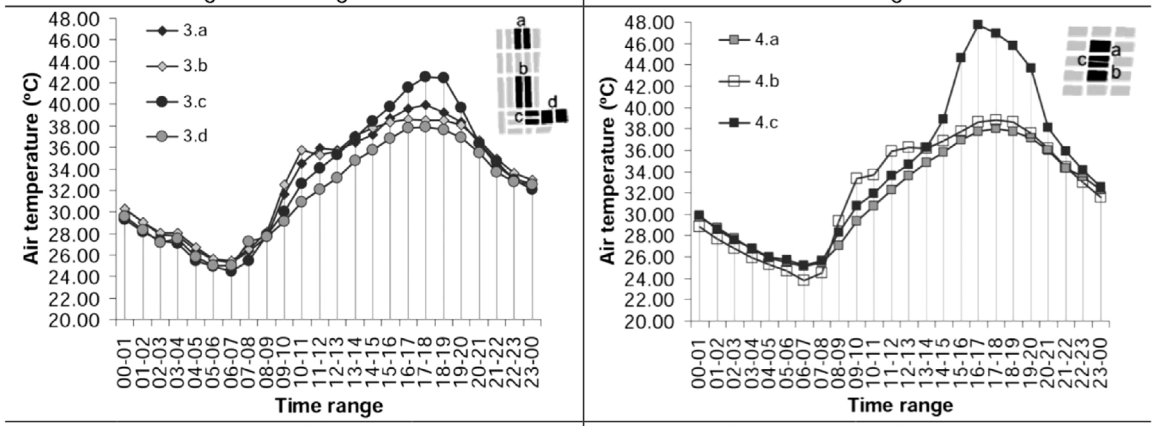

Case	Maximum	Minimum	Average
3.d	37.9°C	25.0°C	31.7°C
3.b	38.6°C	25.4°C	33.0°C
3.a	40.0°C	25.3°C	32.9°C
3.c	42.6°C	24.5°C	32.9°C

Case	Maximum	Minimum	Average
4.a	38.0°C	25.1°C	31.8°C
4.b	38.8°C	23.8°C	32.3°C
4.c	47.7°C	25.2°C	34.1°C

Fig. 7. Thermal behavior of each UC for 01/15/2014.

both cases (ΔT° 1.b − 1.a = −0.3 °C).

- In the Cul-de-Sac grid, it is observed that (i) during the heating period, it is one of the hottest open-forested cases (40.8 °C), and (ii) during the cooling period, the UC achieves the greatest cooling possibilities (24.1 °C).
- In the rectangular grid, it is observed that (i) during the heating period, the E-W-oriented UC (3.c) has the highest maximum temperature (42.6 °C). In addition, the UC N-S-oriented UC (3.d) has the lowest maximum and average temperatures (37.9 °C and 31.7 °C, respectively). (ii) During the cooling period, these cases have similar behavior (ΔT° 3.c-3.d = −0.5 °C).
- In the reticular grid (case 4), it is observed that (i) during the heating period, the non-forested UC (4.c) has the highest maximum air temperature (47.7 °C), while in the coolest open-forested case (UC 4.a), this value reaches 38 °C, (ΔT° 4.c-4.a = 9.7 °C). (ii) During the cooling period, all forested cases have lower minimum air temperatures compared to the non-forested case (oriented E-W).

Considering the neighborhood grid, we can see that the multi-azimuthal case has the best thermal behavior during the day and at night. By comparing the compact-non forested UC with the coolest forested case (1.b), we can see a difference of 10.2 °C in maximum temperatures, 1.7 °C in minimum temperatures and 2.5 °C in average temperatures. These results highlight the need of shade within the urban canyon that the grid form must provide. Another observation is that the compact-non forested model is not suitable for low-density areas (houses of 3 m height) in arid cities because a high H/W ratio is required for shade. Additionally, the neighborhoods layouts need to be wide enough to allow for the radiative and convective cooling exchanges that occur mostly at night due to the relationship with the sky. Regarding the behavior of UCs with different azimuths within and between urban forms, we can see a difference of 2 °C in maximum air temperatures in the UCs within the multi-azimuthal grid and a difference of 5 °C between rectangular and multi-azimuthal grids.

Table 3 presents the correlation results. The Pearson values (r) show the relationships between the indicators used for the characterization of the case studies and their thermal behavior. Both morphological study scales (neighborhoods and canyons) were used to define the key variables that influence outdoor thermal behavior. A unified correlation matrix was made with all the indicators used for each characterized study scale.

By analyzing the r values, we can see that minimum air temperature (UHI effect reduction) is related to the neighborhood and urban canyon features (both study scales). This can be seen through street character-

ization indicators (area, length, width and surface) where the correlation coefficients have statistical significance (r = ± 0.50). Meanwhile, maximum (outdoor thermal comfort) and average (energy consumption) air temperatures are related only with the urban canyon features and the forestation of the street. That is:

- With higher block area, greater lengths and widths, more street surface, a larger built-up volume and SVF, and lower street percentage, the minimum air temperature is cooler.
- With greater width, more street surface and a higher quantity of trees, and lower H/W ratio and SVF, the maximum air temperature is cooler.
- With greater width and street surface, and lower H/W ratio, the average air temperature is cooler.

In summary, the layout of an open neighborhood allows energy release mostly due to radiative exchanges as an effect of the spacing of the blocks, houses and trees (higher SVF). This layout is extremely important in arid cities that have clear sky nights with low frequency and intensity of winds, as is the case for Mendoza. Forested canyons help to control the incoming solar radiation by means of tree canopies during the day.

4.2. Thermal behavior relationships between urban neighborhood grids, downtown and peripheral points

Fig. 8 shows the thermal behavior of the four peripheral points and the downtown, as well as their SVFs (their location within the MMA is shown in Fig. 2). The North sector registered the highest maximum air temperature (42.6 °C) and the lowest minimum (21.4 °C). The downtown point registered the coolest maximum air temperature (36.8 °C) and the highest minimum (26.3 °C). These behavioral differences between the peripheries and downtown are a result of several factors, including but not limited to the amount of built- up areas and the anthropogenic heat generation (e.g., transportation and air conditioning use) that exists within a city (Ahmed et al., 2013). In terms of

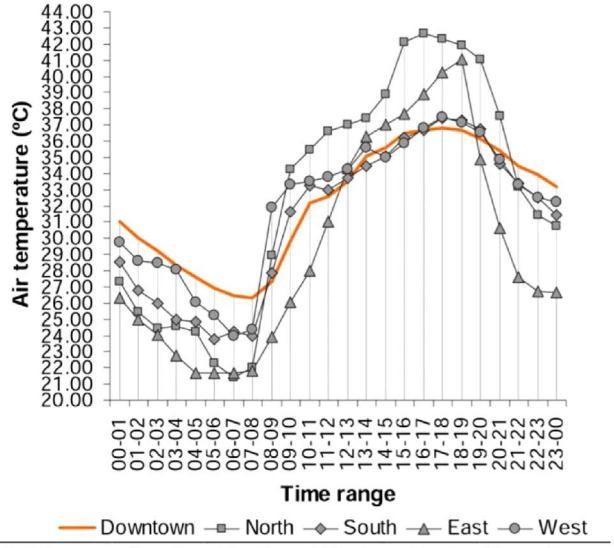

Points	South	North	West	East	Downtown
Maximum	37.4°C	42.6°C	37.5°C	41.8°C	36.8°C
Minimum	23.8°C	21.4°C	24.0°C	21.5°C	26.3°C
Average	31.2°C	32.6°C	32.0°C	31.7°C	32.1°C
SVF	0.91	0.82	0.92	0.89	0.13

Fig. 8. Thermal behavior of peripheral and downtown points.

habitability, the downtown behavior is positive. However, at night, this area suffers from the worst scenario of UHI.

Fig. 9 shows the thermal differences between the coolest urban canyons of each neighborhood and the downtown and the peripheral points.

An analysis of the downtown area shows that:

- For maximum T°, the downtown is always cooler, and the Cul-de-Sac case (2) demonstrates the warmest difference (ΔT° = 4 °C). As was expected, the downtown remains cooler due to the combined effects of shade and thermal inertia (SVF = 0.13, tall buildings and first magnitude trees).
- For minimum T°, the urban neighborhoods always remain cooler, the multi-azimuthal case (1.b) demonstrates the coolest difference (ΔT° = 2.8 °C). This allows night time cooling due to the increase of the sensible heat transference to the sky (UHI effect reduction).
- For average air temperatures, three of the urban canyons (1.b, 3.d and 4.a) are cooler, and the multi-azimuthal case (1.b) demonstrates the coolest difference (ΔT° = 0.5 °C). Energy is saved by natural cooling of the houses in these canyons.

The analysis with the peripheries shows that:

- For maximum T°, the Cul-de-Sac and the reticular grids remain cooler. The reticular case (4.a) demonstrates the coolest difference (ΔT° = 4.6 °C).
- For minimum T°, three of the urban canyons (3.d, 4.a and 2) are warmer, but the multi-azimuthal case (1.b) remains the coolest (ΔT° = 0.3 °C).
- For average air temperatures, two of the urban canyons (1.a and 2) are warmer, but the reticular case (4.a) remains the coolest (ΔT° = 0.8 °C).

In summary, we can see how the increase of built-up areas has an impact on the cooling possibilities of the urban canyons and the downtown compared to the thermal behavior of the peripheries. This effect is more intense in the North-East sector of the MMA (ΔT° min = 3.7 °C).

4.3. Influence of the urban form on energy consumption for cooling

With the values of Table 2, the Qaux is estimated using PREDISE. Fig. 10 shows the electricity needed for cooling the houses according to their façade orientation for each urban canyon configuration. As a result, the houses located in the compact-non forested scheme consume up to 65% more electricity than the houses in the open-forested scheme.

4.4. Conclusions and observations

The study results found that the multi-azimuthal neighborhood grid remains the coolest and that the compact non-forested canyon is the hottest streetscape. Strong correlations were found between minimum air temperature (UHI reduction) and the combined effects of the neighborhood grid and the urban canyon configuration (both study scales). On the other hand, maximum and average air temperatures are related only with the urban canyon configuration and the forestation of the street. The compact-non forested canyon compromises nighttime cooling because of the excessive rise in temperature during the day and the difficulty of cooling at night due to its narrow streets. This streetscape intensifies the UHI effect (ΔT° minimum = 1.7 °C), diminishes outdoor thermal comfort (ΔT° maximum = 10.2 °C) and increases energy consumption (ΔT° average = 2.5 °C, 65% more consumption). These factors are why consciously planning sustainable urban built environments in arid zones is advantageous. We highlight that urban planning must combine the form of the urban neighborhood grids and the design of the urban canyons to select suitable built-up

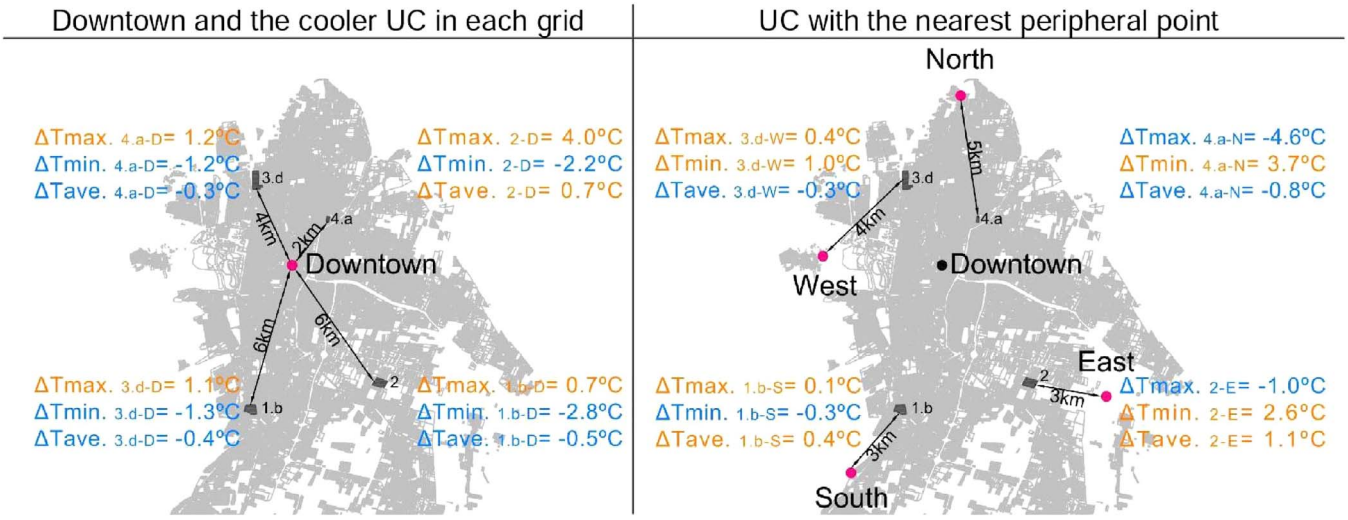

Fig. 9. Thermal differences between the downtown, urban neighborhoods, and the peripheral points.

Streetscape	Compact non-forested (4.c)	Open-forested (1.b)	Σ energy consumption
South façades	121 kWh	71 kWh	50 kWh
North façades	123 kWh	77 kWh	46 kWh
Δ energy consumption	244 kWh	148 kWh	96 kWh
Energy consumption graph	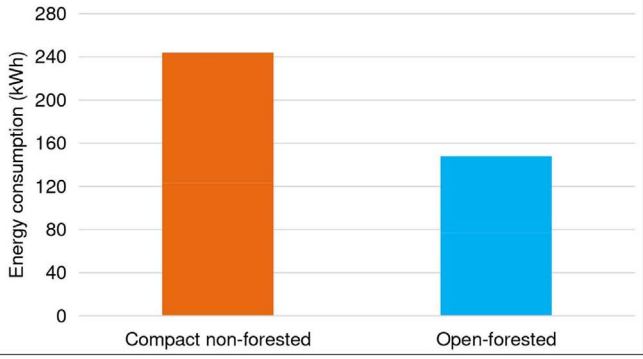		

Fig. 10. Electricity consumption for cooling the housing in both urban schemes.

forms. These observations need to be further studied and diagnosed. Future research should generate recommendations and guidelines for urban designers and planners to help them select a more environmentally responsible urban layout.

Acknowledgments

This work was supported by the Agencia Nacional de Promoción Científica y Tecnológica (ANPCYT) [grant numbers PICT 2011-0611]; and the Consejo Nacional de Investigaciones Científicas y Técnicas (CONICET) [grant number PIP 2011-00640].

References

Ahmed, B., Kamruzzaman, M., Zhu, X., Shahinoor Rahman, Md., & Keechoo, C. (2013). Simulating land cover changes and their impacts on land surface temperature in Dhaka, Bangladesh. *Remote Sensing*, *5*, 5969–5998. http://dx.doi.org/10.3390/rs5115969.

Alchapar, N., & Correa, E. (2015). *Comparison the performance of different facade materials for reducing building cooling needs. Eco-efficient materials for mitigating building cooling needs*. Cambridge: Woodhead Publishing, 155–194.

Córica, L., & Pattini, A. (2009). Study of the potential of natural light in low and high density urban environments in the oasis city of Mendoza, in summer. *Journal of Light & Visual Environment*, *33*, 2.

Correa, E., de Rosa, C., & Lesino, G. (2008). Urban heat island effect on heating and cooling degree day's distribution in Mendoza's metropolitan area. Environmental costs. In Sociedade Portuguesa de energia solar (SPES) (Vol. Ed.), *Proceedings of the 1 st international conference on solar heating, cooling and buildings (EUROSUN 2008). 2*, (pp. 951–958).

Correa, E., Ruiz, M. A., & Cantón, M. A. (2010). Urban forest structure and thermal comfort in oasis cities of arid zones. *Ambiente construído*, *10*, 119–137. http://dx.doi.org/10.1590/S1678-86212010000400009.

Di Rienzo, J., Casanoves, F., Balzarini, M., González, L., Tablada, M., & Robledo, W. (2011). *InfoStat v. 2011*. Argentina: Grupo InfoStat, FCA, Universidad Nacional de

Córdoba.
EPRE, Ente Provincial de Regulación Eléctrica (2014). *Informe técnico de evolución de la demanda de enero de 2014*. [accessed 10 April 2015].
Hernández, A. (2002). PREDISE. Un novedoso y práctico programa de evaluación térmica de edificios. *Avances en energías renovables y medio ambiente*, *6*(2), 61–66 Retrieved from www.unsa.edu.ar/alejo/predise/#link1.
INDEC, Instituto Nacional de Estadísiticas y Censos (2014). *Censo nacional de población, hogares y viviendas*. Argentina: INDEC. http://www.censo2010.indec.gov.ar/.
IPV, Instituto Provincial de la Vivienda de Mendoza (2014). *Censo nacional de población, hogares y viviendas*. Argentina: IPV. http://www.censo2010.indec.gov.ar/.
Jo, H., Goleen, J. S., & Shin, S. W. (2009). Incorporating built environment factors into climate change mitigationstrategies for Seoul, South Korea: A sustainable urban systems framework. *Habitat Internacional*, *33*, 267–275.
Jusuf, S. K., Wong, N. H., & Hagen, E. (2007). The influence of land use on the urban heat island in Singapore. *Habitat Internacional*, *31*(2), 232–242. http://dx.doi.org/10.1016/j.habitatint.2007.02.006.
Lin, T. P., Matzarakis, A., & Hwand, R. L. (2011). Shading effect on long-term outdoor thermal comfort. *Building and Environment*, *45*. http://dx.doi.org/10.1016/j.buildenv.2009.06.002 [213-211].
Maile, T., Fischer, M., & Bazjanac, V. (2007). *Building energy performance simulation tools a life-cycle and interoperable perspective publication type. Working paper*.
Marshall, S. (2005). *Streets and patterns*. London and New York: Spon Press [ISBN 0415317509].
Middel, A., Häb, K., Brazel, A. J., Martin, C. A., & Guhathakurta, S. (2014). Impact of urban form and design on mid-afternoon microclimate in Phoenix Local Climate Zones. *Landscape and Urban Planning*, *122*, 16–28. http://dx.doi.org/10.1016/j.landurbplan.2013.11.004.
Middel, A., Chhetri, N., & Quay, R. (2015). Urban forestry and cool roofs: Assessment of heat mitigation strategies in Phoenix residential neighborhoods. *Urban Forestry & Urban Greening*, *14*, 178–186.
Minghong, T., & Xiubin, L. (2015). Quantifying the effects of settlement size on urban heat islands in fairly uniform geographic areas. *Habitat International*, *49*, 100–106.
Oke, T. R. (1982). The energetic basis of the urban heat island. *Quarterly Journal Royal Meteorological Society*, *108*(45), 1–24. http://dx.doi.org/10.1002/qj.49710845502.
Oke, T. R. (2004). *IOM Report No. 81, WMO/TD No. 1250: Initial guidance to obtain representative meteorological observations at urban sites*Geneva: WMO.
Rodrigues, E., Amaral, A. R., Gaspar, A. R., Gomes, Á., da Silva, M. C. G., & Antunes, C. H. (2015). GerAPlanO – A new building design tool: design generation, thermal assessment and performance optimization. *Energy for sustainability 2015 sustainable cities: designing for people and the planet*.
Ruiz, M. A., & Correa, E. N. (2014). Suitability of different comfort indices for the prediction of thermal conditions in tree-covered outdoor spaces in arid cities. *Theor. Appl. Climatol*, *122*, 69–83. http://dx.doi.org/10.1007/s00704-014-1279-8.
Ruiz, M. A., Sosa, M. B., Correa, E., & Cantón, M. A. (2015). Suitable configurations for forested urban canyons to mitigate the UHI in the city of Mendoza, Argentina. *Urban Climate*, *14*, 197–212. http://dx.doi.org/10.1016/j.uclim.2015.05.005.
Salamanca, F., Georgescu, M., Mahalov, A., Moustaoui, M., & Wang, M. (2014). Anthropogenic heating of the urban environment due to air conditioning. *Journal of Geophysical Research: Atmospheres*, *119*, 1–17. http://dx.doi.org/10.1002/2013jd021225.
Sanusi, R., Johnstone, D., May, P., & Livesley, S. (2016). Street orientation and side of the street greatly influence the microclimatic benefits street trees can provide in summer. *Journal of Environmental Quality*, *45*, 167–174.
Shahraki, S., Sauri, D., Serra, P., Modugno, S., Seifolddini, F., & Pourahmad, A. (2011). Urban sprawl pattern and land-use change detection in Yazd, Iran. *Habitat International*, *35*, 521–528. http://dx.doi.org/10.1016/j.habitatint.2011.02.004.
Shashua-Bar, L., & Hoffman, M. E. (2003). Geometry and orientation aspects in passive cooling of canyon streets with trees. *Energy and Buildings*, *35*, 61–68. http://dx.doi.org/10.1016/s0378-7788(02)00080-4.
Stewart, I. D., & Oke, T. R. (2012). Local climate zones for urban temperature studies. *Bulletin of the American Meteorological Society*, *92*, 1879–1900. http://dx.doi.org/10.1175/bams-d-11-00019.1.
Stocco, S., Cantón, M. A., & Correa, E. (2013). Evaluation of summer thermal conditions and the environmental efficiency of different urban square designs in Mendoza, Argentina. *Hábitat Sustentable*, *3*(2), 19–34.
Stone, B., Hess, J., & Frumkin, H. (2010). Urban form and extreme heat events: Are sprawling cities more vulnerable to climate change than compact cities? *Environmental Health Perspectives*, *10*, 1425–1428. http://dx.doi.org/10.1289/ehp.0901879.
UN-Habitat Working Paper (2013). *The relevance of street patterns and public space in urban areas*.
UN-Habitat World Cities Report (2016). *Urbanization and development: emerging futures*.
Weather Underground. (2014). Retrieved from https://espanol.wunderground.com/.
Wong, J., & Siu-Kit, L. (2013). From the 'urban heat island' to the 'green island'?: A preliminary investigation into the potential of retrofitting green roofs in Mongkok district of Hong Kong. *Habitat International*, *39*, 25–35.
Wu, J. G. (2014). Urban ecology and sustainability: The state-of-the-science and future directions. *Landscape and Urban Planning*, *125*, 209–221. http://dx.doi.org/10.1016/j.landurbplan.2014.01.018.
Zhao, C., Fu, G., Liu, X., & Fu, F. (2011). Urban planning indicators, morphology and climate indicators: A case study for a north-south transect of Beijing, China. *Building and Environment*, *46*, 1174–1183.